ELSEVIER

International Journal of Pharmaceutics 135 (1996) 31–42

international journal of pharmaceutics

Research papers

Calorimetric method for rapid determination of critical water vapor pressure and kinetics of water sorption on hygroscopic compounds

Lee D. Hansen[a,*], John W. Crawford[a], Darren R. Keiser[a], Ray W. Wood[1b]

[a]*Department of Chemistry and Biochemistry, Brigham Young University, Provo, UT 84602, USA*
[b]*Pharmaceutical Sciences R and D, Baxter Healthcare Corporation, Route 120 and Wilson Road, Round Lake, IL 60073, USA*

Received 28 December 1994; revised 24 March 1995; accepted 26 June 1995

Abstract

A rapid method for determining the equilibrium water vapor pressure over a hydrate or saturated solution has been developed. The vapor space over the sample in an isothermal, heat conduction calorimeter is titrated with water vapor generated by continuously scanning the temperature of a container of water outside the calorimeter. The rate of heat production in the sample, which is proportional to the rate of water sorption by the sample, remains very small until the critical water vapor pressure is reached. The heat rate (ϕ) increases markedly and is proportional to water vapor pressure above the critical water vapor pressure. The change in $d\phi/dp_{H2O}$ signals the appearance of a new phase. The method was tested with NaBr, $NaHSO_4$, Na_2SO_4, NH_4Cl and $(NH_4)_2SO_4$ at 24, 34, 44 and 54°C. Critical water vapor pressures determined are all within 2 torr of those predicted from literature data. ΔH values for the reaction with $H_2O(g)$, calculated from the temperature dependence of the critical water vapor pressure, are close to the enthalpy change for condensation of water and agree with literature data. In the regions of the titration curve before and after a phase change, the value of $(d\phi/dp_{H2O})$ is shown to be equal to the product of the rate constant for water sorption, a function of sample surface properties, and ΔH for the reaction. Values of $(d\phi/dp_{H2O})$, both before and after phase transitions, were determined at the four temperatures. The Arrhenius activation energy for water sorption is approximately zero for all the reactions studied.

Keywords: Calorimetry; Water vapor; Hydration; Kinetics; Sodium bromide; Sodium hydrogen sulfate; Sodium sulfate; Ammonium chloride; Ammonium sulfate

1. Introduction

Controlling the sorption of water vapor from air is crucial to quality control in manufacturing of some pharmaceuticals. Some materials are decomposed and the physical properties of many materials are altered by water sorbed from the air.

* Corresponding author. Tel.: +801 378 2040.
[1] Present address: Nanosystems, Collegeville, PA 19355, USA.

PII S0378-5173(96)04494-8

Properties such as chemical stability, flowability, lubricity, compressibility, density, particle size and shape, and solubility of powders can be altered by sorbed water. Transport properties of polymers and the handling properties of drugs and excipients can be affected by sorbed water. To avoid such decomposition and alteration in properties, packaging and conditions of storage and handling must be established through measurement of the extent and rate of reaction of the material with water vapor (Carstensen, 1977). Quickly characterizing the reaction of a material with water vapor in the early stages of formulation or for quality control of variable raw materials are particular needs. Currently available procedures (Carstensen, 1977; Van Campen et al., 1980; Umprayn and Mendes, 1987) for measuring water sorption are simple, but labor intensive and sometimes require weeks to months to obtain results. The sorption of water on solids is commonly measured by placing the solid in a hygrostat with a known water vapor pressure, p_{H2O}, and weighing the solid at intervals or continuously until a constant weight is reached. This equilibrium moisture content (e.m.c.) method is slow because it requires that equilibrium be attained. Because it is slow, water sensitive materials can decompose during the experiment. Also, determining when equilibrium has been reached is not simple. The assumption that equilibrium has been reached when the hydrated sample reaches a constant weight is not necessarily correct. Constant weight simply means the rate of water sorption has become too slow to detect. Equilibrium should be approached from both directions in e.m.c. measurements, but this is not always practical.

Another approach to characterizing the reaction of water with a sorbent is to measure the rate of water sorption as a function of p_{H2O}. This approach has the advantage of speed. Since attainment of equilibrium is not required, an entire experiment can be done in a few hours. Furthermore, the shape of a plot of the rate of reaction versus p_{H2O} contains information about the nature of the reaction. In a sorption system with no phase change, the rate will increase continuously with increasing p_{H2O}. In a purely phase change system, the rate will be zero below p^c_{H2O} and abruptly begin to increase at $p_{H2O} > p^c_{H2O}$. Above p^c_{H2O} the rate will be proportional to a function of $p_{H2O} - p^c_{H2O}$ (Van Campen et al., 1983a; Van Campen et al., 1983b; Van Campen et al., 1983c), and thus will increase rapidly as p_{H2O} increases. The disadvantages of the rate method compared to the e.m.c. method for determining p^c_{H2O} are that no data on stoichiometry are obtained and very slow reactions or reactions with a large variation in Gibbs free energy may be missed.

The objective of this study is to develop a rapid technique to (a) characterize the nature of the reaction of water with hygroscopic compounds, (b) determine the water vapor pressure in equilibrium with new phases appearing in the sample as the water vapor pressure is increased, and (c) determine the kinetics of water sorption. In the method described here, the water vapor pressure in the atmosphere in contact with the sample is continuously increased by upward scanning of the temperature of a container of water and transporting the vapor to the sample by a gas stream bubbled through the water. The rate of reaction of the water with the sample is detected with an isothermal, heat conduction calorimeter. Phase changes in the sample appear as abrupt changes in the rate of change of the heat production rate with p_{H2O}. Sorption of water not accompanied by a phase change appears as a gradually increasing rate with increasing p_{H2O}.

The equipment and methods were tested with five inorganic compounds, i.e. NaBr, $NaHSO_4$, Na_2SO_4, NH_4Cl and $(NH_4)_2SO_4$, with well characterized hydrates and/or saturated solutions having water vapor pressures in the range of interest, i.e. about 5–100 torr (1 torr = 1 mm Hg = 133.322 Pa). Determinations were done at 24, 34, 44 and 54°C. The results show that p^c_{H2O} values accurate to within 2 torr can be determined by this method. Data on the dependence of the rate of water sorption on p_{H2O} and temperature were also obtained in the course of the study.

2. Materials and methods

2.1. Materials

NaBr (Fisher, ACS), $NaHSO_4.H_2O$ (Baker, reagent), Na_2SO_4 (Baker, reagent), NH_4Cl (Mallinckrodt, ACS) and $(NH_4)SO_4$ (Baker, reagent) were dried overnight in a vacuum oven at 110–120°C and then stored at room temperature in a desiccator with Drierite.

2.2. Methods

A temperature scanning block (Al, 3 inch cube) with four wells, each holding a glass bottle with about 10 mL of water was constructed. The block temperature was measured with an LM335 precision temperature sensor (10 mV K^{-1}, National Semiconductor) calibrated against an NIST traceable platinum thermometer (Hart Scientific model 1004) placed in one of the water bottles. The block controller was programmed by an IBM XT computer which was also used to collect block temperature and calorimetric data. The scanning block was mounted on the chassis of a Hart Scientific model 7707 differential, heat conduction, scanning calorimeter (DSC). The block and the opening into the calorimeter measuring cells were surrounded by a box constructed of 2 inch thick styrofoam. A heater mounted on the inside of the box lid heats the air in the box above the temperature of the sample in the calorimeter to prevent condensation of water in the gas flow lines between the water bottles and the calorimeter ampules. The box heater was controlled manually with a variac.

In this study, the DSC was operated in the isothermal mode. Isothermal baseline reproducibility without gas flowing is typically ± 5 μW, and the peak to peak noise is less than 1 μW. With gas flowing, both figures are increased, the first to about ± 15 μW and the second to as much as 10 μW.

The DSC has four 1-mL sample chambers with removable ampules. One of the ampules (# 4) is empty, not connected to the gas flow system, and serves as an instrument reference. The data collected are the differences in heat rate between ampule # 4 and each of the other ampules. One of the three sample ampules was sometimes left empty but connected to the gas flow stream to obtain baseline data. The ampules were loaded with sufficient sample to cover the ampule bottom, typically about 50 mg.

The gas flow system consists, in order, of a tank of nitrogen, a two stage pressure regulator (400 psi second stage), 3 feet of 50 μm i.d. glass capillary tubing, the water bottles with serum caps in the block, a 0.1 cm^3 spray trap, about 1 foot of 100 μm glass capillary tubing in the insulated chamber directly above the calorimeter, the sample ampules, about 1 foot of 100 μm tubing, and an open vial of water to give visual indication of gas flow. The pressure regulator was set to about 80 psi outlet pressure. At this pressure, the 50 μm capillary delivers a constant flow of about 1 mL/min. Fig. 1 is a schematic of the entire system.

The most difficult part of the experimental procedure developed here is preventing condensation of water in the gas flow lines between the water bottles and the calorimeter ampules. The problem can be avoided by operating the circulating bath about 10°C above the calorimeter temperature, heating the air in the styrofoam enclosure to a temperature above the calorimeter temperature, and being careful to avoid any condition allowing condensation in the gas flow lines between experiments. Operating the circulating bath above the calorimeter temperature ensures that the isothermal shields around the calorimeter are at a higher temperature than the calorimeter, and thus that there will be no condensation of water in the gas flow tubes where they pass through these shields. A hair dryer was sometimes found convenient to preheat and dry the tubes just prior to starting gas flow for an experiment. The bubble trap placed at the lid of the water bottles usually prevents entrained spray droplets from entering the transfer tube, but occasionally a drop will find its way to the calorimeter ampule and ruin an experiment.

An experiment consists of setting the calorimeter sample temperature, setting the temperature of the bath circulating fluid to the calorimeter about 10°C above the calorimeter temperature, cooling the scanning block to the starting temperature, weighing sample into the ampules, placing the

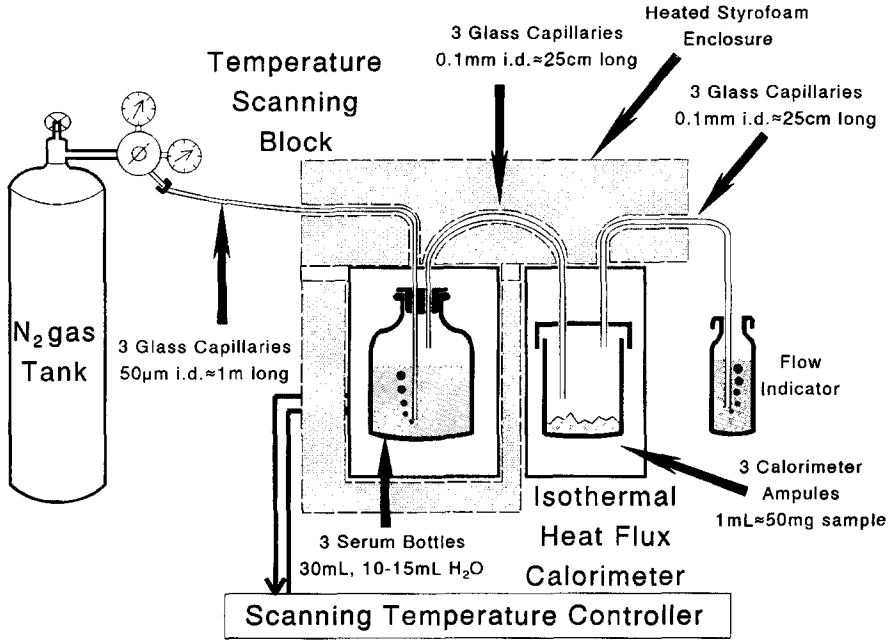

Fig. 1. Schematic diagram of the experimental setup.

ampules into the calorimeter, starting the gas flow, setting the current to the box heater, waiting about 30 min for the calorimeter to stabilize, then starting the program to scan the block temperature. A data set consists of (a) the calorimeter temperature, a single number precise to 0.001°C and accurate to about 0.2 K, (b) block temperatures usually collected at a rate of one per min, precise to 0.001°C and accurate to about ± 2°C in reflecting the water temperature in the bottles in the wells, and (c) sample heat rates matching the block temperatures in time.

Data analysis is done in two steps. First, the block temperatures are converted to matching water vapor pressures using literature data (Weast, 1974a). This was conveniently done with equation 1 which fits these data within 0.1 torr over the range from 5 to 60°C.

$$\ln p_{H_2O} = 18.515 - [3855.8/(T°C + 273.15)] - [214690/(T°C + 273.15)^2] \quad (1)$$

(An equation describing p_{H2O} over a wider temperature range is available, but was not discovered until after this work was done; see Hall and Brouillard, 1985.) In the second step, a plot of heat rate versus p_{H2O} is constructed and used to find the critical water vapor pressure, p^c_{H2O}. p^c_{H2O} is determined as the intersection of the two branches of the curve by linear extrapolation.

By subtracting the heat rate data taken on an empty ampule (i.e. a baseline) from the heat rate data taken on a sample, an estimate of the rate of sorption of water on the solid can be obtained. Such a baseline correction was only done in this study in obtaining kinetic data, since baseline correction is not necessary to discern the endpoint at the phase change.

3. Results

3.1. Thermodynamics

Fig. 2 gives examples of the baseline data collected with empty ampules. The general upward slope, i.e. increasing heat rate with increasing block temperature or vapor pressure, is caused by the increasing temperature of the gas stream entering the calorimeter ampules. The increase in

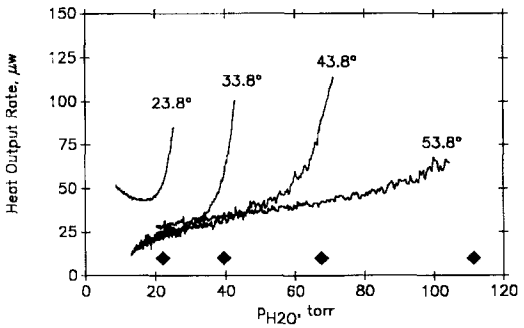

Fig. 2. Results from baseline control experiments with empty ampules in the calorimeter. The saturation vapor pressure of water at each temperature is indicated by the diamonds.

the slope near the saturation pressure is probably due to adsorption of water onto the surface of the calorimeter ampule, i.e. there is incipient condensation. Condensation must of course occur when the scanning block temperature is at or above the calorimeter sample temperature, i.e. at the points indicated by the diamonds in Fig. 2. The absolute value of the baseline depends on the temperatures of the room, the fluid circulating in the calorimeter, and the air in the box over the calorimeter. The dependence on room temperature explains why the baseline at 24°C is more positive than baselines taken with the calorimeter operating above room temperature.

Figs. 3 and 4 graphically show the results of one experiment on NH_4Cl and $(NH_4)_2SO_4$ at each temperature. Baselines have not been subtracted from the data shown. Endpoints at increasing water vapor pressure with increasing sample temperature are readily discernible in the plots.

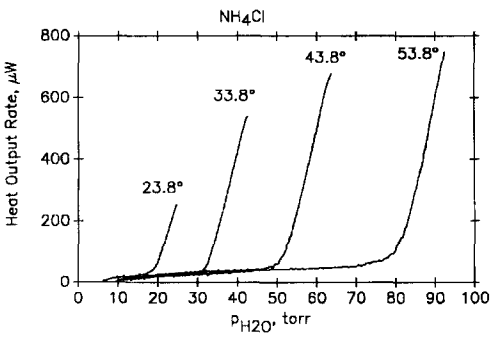

Fig. 3. Example data sets for NH_4Cl.

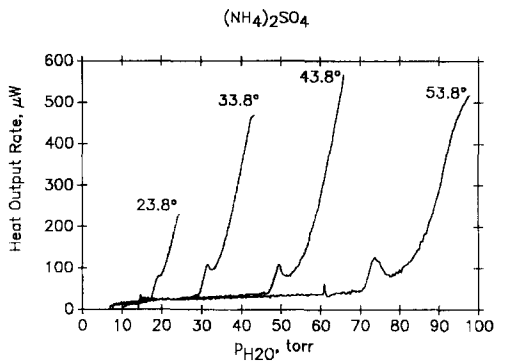

Fig. 4. Example data sets for $(NH_4)_2SO_4$.

NH_4Cl shows one endpoint at the appearance of the saturated solution, and $(NH_4)_2SO_4$ shows two endpoints, the second being for the saturated solution. Note the much larger magnitudes of the vertical scales on Figs. 3 and 4 than on Fig. 2.

Data can also be plotted as a function of relative humidity, h_r. Such a plot for NaBr is shown in Fig. 5. Note that construction of ϕ versus h_r plots from ϕ versus p_{H2O} plots as shown in Figs. 3 and 4 only requires division of the p_{H2O} data for each plot at a given temperature by the saturation vapor pressure of pure water at each temperature. Such a division by a constant does not change the shape of the plot, it only changes the values on the horizontal axis.

Heat rate versus p_{H2O} data for $NaHSO_4$ and Na_2SO_4 are not shown, but are similar in appearance to that shown for $(NH_4)_2SO_4$ (Fig. 4) and NH_4Cl (Fig. 3), respectively.

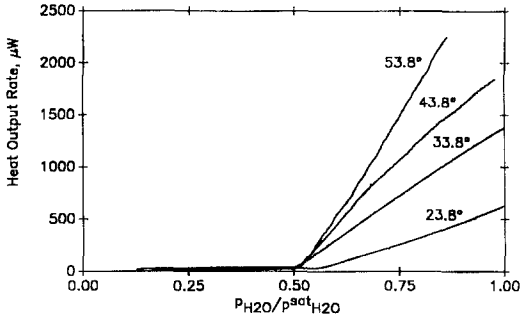

Fig. 5. Rate of heat output from NaBr as a function of relative humidity over the sample.

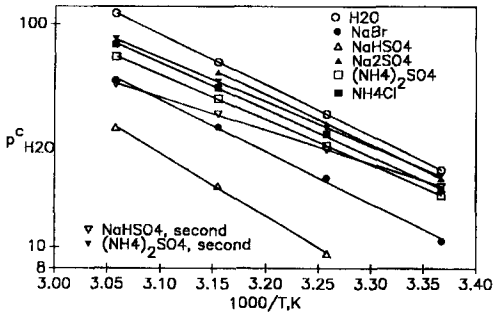

Fig. 6. van't Hoff plot comparing p^c_{H2O} for water and the compounds studied.

Sample sizes from 10 to over 100mg were tested. The smallest samples gave uncertain results because the signal from the hydration reaction was too small, but in general there was little effect of sample size.

Scan rates from 1 to 20°C/h were tested. No differences in results were found at scan rates from 1 to 7°C/h. At scan rates higher than 10°C/h, the endpoint appeared too late, i.e. at erroneously high values of p^c_{H2O}, either because the temperature of the water in the bottles lags behind the block temperature or because the reaction rate is limited by the transport rate of water to the solid sample. At the lower scan rates, six samples can conveniently be studied in a 24-h period. Since materials should be studied at different scan rates to determine whether a reaction is water catalysed, uses water as a reactant, or is slow, it is convenient to run one scan requiring about 8 h during the day and another scan requiring about 16 h during the night.

Fig. 6 is a van't Hoff plot for water and the compounds studied. Within the limits of uncertainty, all of the data in Fig. 6 fall on straight lines, thus showing the reactions have been correctly correlated at the different temperatures. ΔH values calculated from the data in Fig. 6 are given in Table 1 together with literature values. ΔH values calculated in this way are per mole of water and are for the reaction to form the hydrate or for the heat of solution in a saturated solution.

Table 1 gives the p^c_{H2O} values from this study and comparative literature data. The precision of the p^c_{H2O} values ranges from about 0.2 to 2 torr. Because the values in this study and literature values are at different temperatures they are not easily compared in tabular form, but can be readily compared graphically in van't Hoff plots as illustrated in Fig. 7. The p^c_{H2O} values from this study are in reasonable agreement with literature values except for $NaHSO_4$ in which case the literature values are questionable.

The reaction of NH_4Cl with water to form a saturated solution is the only known hydration reaction of this compound. Only one endpoint was found in this study and the p^c_{H2O} values determined are slightly higher, but within 1 torr of literature values for the water vapor pressure in equilibrium with the saturated solution. The ΔH value from this study (-40 kJ/mol) is in good agreement with the literature value (-42 kJ/mol) (Wagman et al., 1982).

The only hydration reaction reported in the literature for $(NH_4)_2SO_4$ is formation of the saturated solution. Two endpoints were found for $(NH_4)_2SO_4$, however. Assuming the second endpoint is the saturated solution, the first endpoint must be a hydrate. It could be metastable or may only exist too close to the deliquescence point to have been discovered previously. A more likely possibility is that the drying procedure created an acid salt such as NH_4HSO_4 by loss of ammonia from the surface of the crystals, and the first endpoint is for reaction of the acid salt with water. This latter explanation agrees with the appearance of the data in Fig. 4 since the first endpoint represents reaction of only a small amount of material as shown by the small amount of total heat released. The small amount of reaction is most obvious at the higher temperatures where the first reaction ends before the second begins. It is interesting that this method clearly shows such surface contamination effects. The p^c_{H2O} values from the second endpoint are slightly higher than, but within about 1 torr of literature values for the equilibrium vapor pressure over the saturated solution. The ΔH value from this study (-38 kJ/mol) is low compared to the literature value of -43 kJ/mol (Wagman et al., 1982).

Because they all form crystalline hydrates, two endpoints are expected for NaBr below 51°C, for Na_2SO_4 below 32.5°C, and for $NaHSO_4$ at all

Table 1
Reactions, equilibrium vapor pressures and enthalpy changes for hydration of the compounds in this study with water vapor

Reaction[a]	T,°C	$p^{e}_{H_2O}$,torr[a,b]	$-\Delta H$ kJ/mol H_2O (T°C)
$NH_4Cl(c)+H_2O(g)\rightarrow NH_4Cl(aq.,ss)$	20	13.8ss[c]	40.3 (van't Hoff, 24–54; this study)
	23.8	18 ± 0.9(3)	42.1 (aq. in $8H_2O$, 25[d])
	25	18.6ss[c]	
	30	24.4ss[c]	
	33.8	32.0 ± 0.1(5)	
	43.8	51.6 ± 0.2(3)	
	53.8	81.0 ± 0.6(3)	
(First endpoint)			
$(NH_4)_2SO_4(c)+?H_2O(g)$	23.8	17.1 ± 0.4(4)	38.5 (van't Hoff 24–54; this study)
$\rightarrow (NH_4)_2SO_4\cdot ?H_2O(c)$			
or NH_4HSO_4	33.8	28.4 ± 0.4(5)	
$+?H_2O(g)\rightarrow NH_4HSO_4\cdot ?H_2O$(c or aq., ss)			
	43.8	46.2 ± 0.6(3)	
	53.8	71.4 ± 0.8(3)	
(Second endpoint)			
$(NH_4)_2SO_4(c)+H_2O(g)$	20	13.9ss[e], 14.1ss[c]	38.1 (van't Hoff, 24–54; this study)
$\rightarrow (NH_4)_2SO_4$(aq.,ss)			
	23.8	20.9 ± 0.6(3)	43.4 (aq. in $10H_2O$, 25[d])
	25	18.8ss[e], 19.1ss[c]	
	30	25.1ss[e], 25.6ss[c]	
	33.8	33.9 ± 0.2(5)	
	35	33.3ss[e]	
	40	43.7ss[e]	
	43.8	55.1 ± 0.6(3)	
	53.8	85.7 ± 0.4(3)	
(First endpoint)			
$NaHSO_4(c)+H_2O(g)\rightarrow NaHSO_4\cdot H_2O(c)$	23.8	<7(3)	54.2 (van't Hoff 34–54; this study)
	25	12.3c[d]	54.4 (25[d])
	33.8	9.3 ± 0.3(4)	
	43.8	18.8 ± 0.1(3)	
	53.8	34.2 ± 0.3(3)	
(Second endpoint)			
$NaHSO_4(c)+H_2O(g)\rightarrow NaHSO_4$(aq.,ss)	20	9.0ss[c], 9.1ss[f]	28.5 (van't Hoff 34–54; this study)
or	23.8	18.7 ± 0.9(3)	44.3 (aq. in 10 H_2O, 25[d])
$NaHSO_4\cdot H_2O(c)+H_2O(g)$			
$\rightarrow NaHSO_4$(aq.,ss)			
	33.8	27.3 ± 4.0(2)	or 43.2 (aq. in 10 H_2O, 25[d])
	43.8	39.5 ± 2.8(3)	
	53.8	53.6 ± 2.3(3)	
$NaBr(c)+2H_2O(g)\rightarrow NaBr\cdot 2H_2O(c)$	20	10.1ss[c], 10.4ss[g], 10.0ss[e], 10.2ss[f]	46.1 (van't Hoff 24–44; this study)
or $NaBr(c)+H_2O(g)\rightarrow NaBr$(aq.,ss)	23.8	10.6 ± 0.2(11)	44.5 (van't Hoff 24–54; this study)
	25	8.7c[d], 13.7ss[g], 13.5ss[e]	53.6 (25[d])
	30	18.1ss[e], 17.8ss[g]	
	33.8	20.4 ± 0.8(3)	
	35	22.8ss[g], 24.0ss[e]	
	40	31.5ss[e], 29.4ss[g]	
	43.8	34.4 ± 0.3(3)	
	45	37.4ss[g]	
	50	47.1ss[g]	

Table 1 (contd.)

Reaction[a]	T,°C	p^c_{H2O},torr[a,b]	$-\Delta H$ kJ/mol H_2O (T°C)
($NaBr \cdot 2H_2O$ converts to anhydrous NaBr in contact with H_2O(l) above 51°C[h])			
$NaBr(c) + H_2O(g) \rightarrow NaBr(aq.ss)$	53.8	55.8 ± 0.7(4)	44.6 (aq. in $6.5H_2O$, 25[d])
$Na_2SO_4(c) + 10H_2O(g)$	20	16.1ss[c]	42.7 (van't Hoff 24–44; this study)
$\rightarrow Na_2SO_4 \cdot 10H_2O(c)$			
or $Na_2SO_4(c) + H_2O(g) \rightarrow Na_2SO_4(aq.,ss)$	23.8	20.4 ± 0.2(4)	52.2 (25[d])
	25	19.4c[d]	
($Na_2SO_4 \cdot 10H_2O$ converts to anhydrous Na_2SO_4 in contact with H_2O(l) above 32.5°C[h])			
$Na_2SO_4(c) + H_2O(g) \rightarrow Na_2SO_4(aq.,ss)$	33.8	35.6 ± 1.5(3)	44.5 (aq. in $18H_2O$, 25[d])
	43.8	60.7 ± 0.8(3)	
	53.8	>100(3)	

[a]Abbreviations: c, crystalline; g, gas; ss, saturated solution; aq, aqueous.
[b]Uncertainties are given as the standard deviation of the mean of the number of data points given in parentheses after the uncertainty.
[c]Weast, 1974b.
[d]Wagman et al., 1982.
[e]Rockland, 1960.
[f]Carstensen, 1977.
[g]Nyqvist, 1983.
[h]Linke, 1965.

temperatures used in this study (See Table 1). Only $NaHSO_4$ shows two endpoints, the other two compounds show only one. The single endpoints observed for NaBr and Na_2SO_4 at temperatures where the hydrates exist are probably a combination of the two reactions since the p^c_{H2O} values of the two endpoints are only about 4 torr apart in both cases.

The first endpoint for $NaHSO_4$ is where the reaction to form the monohydrate begins, and the second endpoint occurs where the saturated solution begins to form. The single literature value for p^c_{H2O} for formation of the monohydrate is about 7 torr too high compared with the results of this study. However, the literature value probably has a large uncertainty because it is calculated from tabulated $\Delta G°$ values (Wagman et al., 1982). The ΔH value for formation of the monohydrate, -54 kJ/mol from this study, is the same as the literature value (Wagman et al., 1982). The p^c_{H2O} value for the saturated solution of $NaHSO_4$ at 20°C extrapolated from data from this study appears to be about 4 torr higher than the two literature values which are of unknown uncertainty. The ΔH value from this study for formation of the saturated solution of $NaHSO_4$ is too small by about 15 kJ/mol when compared to the literature value (Wagman et al., 1982). The discrepancy may be due to errors in the sparse literature data or inherent in the van't Hoff treatment of our data. Note that the van't Hoff treatment gives the heat for solution in saturated solution.

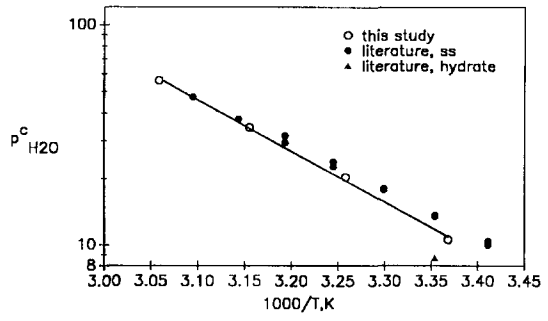

Fig. 7. van't Hoff plot for NaBr comparing literature data (see Table 1) to data from this study.

The p^c_{H2O} results for NaBr and Na_2SO_4 from this study are within 2 torr of the literature value no matter which reaction is occurring at the endpoint. The ΔH values from this study are in good agreement with the literature values for both NaBr and Na_2SO_4 (Wagman et al., 1982) if the

Table 2
Kinetics of $H_2O(g)$ uptake

Temperature °C	Critical relative humidity[a] $h_r^c = p_{H2O}^c/p_{H2O}^{sat}$%		$kA\Delta H = d(\phi,\mu W)/d(P_{H2O}, torr)$		
			Pre-slope[b,c]	Post-slope[b,d]	
	First	Second		First	Second
NH_4Cl					
23.8	81.4 ± 4.1		1.2 ± 0.4 (3)	47 ± 3 (3)	
33.8	81.1 ± 0.3		1.2 ± 0.2 (5)	52 ± 1 (5)	
43.8	76.4 ± 0.3		0.9 ± 0.2 (3)	55 ± 1 (3)	
53.8	72.7 ± 0.5		0.4 ± 0.1 (3)	57 ± 2 (3)	
NaBr					
23.8	47.9 ± 0.9		2.4 ± 0.5 (9)	65 ± 3 (10)	
33.8	51.7 ± 2.0		0.8 ± 0.2 (3)	71 ± 11 (3)	
43.8	50.9 ± 0.4		0.6 ± 0.1 (3)	71 ± 1 (3)	
53.8	50.1 ± 0.6		0.3 ± 0.1 (4)	55 ± 1 (4)	
$(NH_4)_2SO_4$					
23.8	77.3 ± 1.8	94.5 ± 2.7	2.0 ± 0.8 (4)	39 ± 4 (4)	40 ± 2 (3)
33.8	72.0 ± 10.0	85.9 ± 0.5	0.7 ± 0.1 (5)	36 ± 1 (5)	49 ± 2 (5)
43.8	68.4 ± 0.9	81.6 ± 0.9	0.6 ± 0.0 (3)	38 ± 6 (3)	41 ± 6 (3)
53.8	64.1 ± 0.7	76.9 ± 0.4	0.4 ± 0.1 (3)	29 ± 4 (2)	33 ± 8 (3)
$NaHSO_4$					
23.8		84.6 ± 4.1		55 ± 7 (3)	41 (1)
33.8	23.6 ± 0.8	69.2 ± 10.1	8.2 ± 1.9 (4)	66 ± 2 (4)	65 ± 1 (2)
43.8	27.8 ± 0.1	58.5 ± 4.1	1.7 ± 0.1 (3)	68 ± 2 (3)	62 ± 1 (3)
53.8	30.7 ± 0.3	48.1 ± 2.1	1.0 ± 0.1 (3)	70 ± 3 (3)	43 ± 2 (3)
Na_2SO_4					
23.8	92.3 ± 0.9		3.7 ± 1.6 (4)	43 ± 5 (4)	
33.8	90.2 ± 3.8		0.8 ± 0.2 (3)	51 ± 3 (3)	
43.8	89.8 ± 1.2		0.9 ± 0.4 (3)	40 ± 9 (3)	

[a]Calculated from data in Table 1.
[b]Uncertainties are given as the standard deviation of the mean of the number of data points given in parentheses.
[c]Slope below the critical relative humidity.
[d]Slope above the critical relative humidity.

reaction is assumed to be solution of the anhydrous salt to form the saturated solution.

The critical relative humidity at each temperature is given in Table 2. Note that h_r^c is invariant with temperature within the limit of error for NaBr and Na_2SO_4, decreases with temperature for NH_4Cl and $(NH_4)_2SO_4$, and increases with temperature for $NaHSO_4$. Whether and which direction h_r^c (= p_{H2O}^c/p^{sat} for pure water) changes with temperature depends on the relative changes with temperature of the water vapor pressure over the hydrate or saturated solution and over pure water. The temperature dependencies of the vapor pressures are in turn related to the enthalpy changes of the condensation reactions by the van't Hoff equation. h_r^c will increase with temperature if the enthalpy change for formation of the hydrate or saturated solution from liquid water and the solid is exothermic, be invariant with temperature if the enthalpy change is negligible compared with the enthalpy change for condensation of water, and will decrease if the enthalpy change for hydration with liquid water is endothermic. The ΔH values given in Table 1 could thus have been used to predict the changes found for h_r^c.

3.2. Kinetics

The heat rate (ϕ) is proportional to the rate of water sorption dn/dt as shown in equation 2

$$\phi = \Delta H(dn/dt) \quad (2)$$

where ΔH is the enthalpy change for sorption of water. The results in any given region show the heat rate is approximately a linear function of p_{H2O} or humidity. Therefore, the rate of water sorption in the linear regions is described by equation 3

$$dn/dt = kA(p_{H2O} - p^c_{H2O}) \quad (3)$$

where k is a rate constant and A is a constant dependent on the surface properties of the sorbent. Combining equations 2 and 3 gives

$$\phi = kA\Delta H(p_{H2O} - p^c_{H2O}) \quad (4)$$

and taking the derivative with respect to p_{H2O} gives equation 5,

$$(d\phi/dp_{H2O}) = kA\Delta H \quad (5)$$

showing that the slope of a plot of ϕ versus p_{H2O} is equal to kAΔH. Only k is expected to be temperature dependent; A and ΔH should be temperature independent.

Since each region of the titration curve represents a different reaction, there are as many kAΔH values as regions in the curve. For example, physical adsorption occurs below p^c_{H2O} and formation of a saturated solution occurs above p^c_{H2O} in the curves for NH_4Cl (Fig. 3). Table 2 gives the kAΔH values obtained from the slopes in each region of ϕ versus p_{H2O} plots. The value of kAΔH for physical sorption appears to decrease slightly with increasing temperature, but the change may be an instrumental artifact. The value of kAΔH for sorption reactions leading to hydrates or saturated solutions does not appear to change significantly with temperature. For a given material, any change in kAΔH with temperature can be attributed to changes in k, and Arrhenius activation energies can be calculated.

4. Discussion

The data in Table 1 clearly show this new method is a rapid means of precisely determining critical water vapor pressures. The method is valuable for rapidly identifying humidities and temperatures critical for storage and use of water sensitive materials. Also, data plots as shown in Figs. 3 and 4 provide useful data on the nature of the reaction. The sharpness of the endpoints in the curves shown clearly demonstrate the presence of a phase change in these systems. Futhermore, none of the p^c_{H2O} values appear to be dependent on scan rate. However, it is not always simple to determine what reaction is occurring at the endpoint. Auxiliary data are required to define the stoichiometry of the phase change and to assess the accuracy of p^c_{H2O} and ΔH.

The phase change to a hydrate or saturated solution can only occur when p_{H2O} exceeds the equilibrium value, i.e. p^c_{H2O}. No significant change in composition of the sample except adsorption of water can occur until the Gibbs free energy change (ΔG) for the reaction to form the new phase, i.e. a hydrate or saturated solution, becomes negative. Since ΔG for the reaction depends on the water vapor pressure (equation 6),

$$\Delta G = \Delta G^\circ - RTlnp_{H2O} \quad (6)$$

under conditions of increasing water vapor pressure the new phase cannot appear until $\Delta G \leq 0$ and $p_{H2O} \geq p^c_{H2O}$. Thus, only adsorption occurs before the phase change. However, a phase change may be slow and may not be observed until p_{H2O} significantly exceeds p^c_{H2O}. Such an effect should be observed as a decrease in p^c_{H2O} with decreasing scan rate. However, if the reaction is sufficiently slow, it may not be seen at all with this method.

In general, it appears that the method reported in this paper produces p^c_{H2O} values accurate to about 2 torr of water vapor pressure and ΔH values generally good to about 5 kJ/mol. However, if p^c_{H2O} values are close together, not all of the reactions will be seen and assignment of endpoints to a particular reaction will be uncertain. With these caveats in mind, the method does appear to always show an endpoint if there is a

reaction with water. On a practical basis, the method can be used to rapidly define regions of p_{H2O} which require further study.

This method is probably not useful for much more of a range of temperatures than used in this study. At the low end the vapor pressure changes so slowly on an absolute basis that measurements are difficult. At the upper end of the temperature range avoiding unwanted condensation becomes difficult.

The technique described here for determination of p^c_{H2O} should not be confused with a similar appearing measurement of the catalytic effect of water vapor on the rate of crystallization of amorphous materials reported earlier by other workers (Angberg et al., 1992a; Angberg et al., 1992b). Since the kinetics of crystallization of amorphous materials are autocatalytic, such a reaction could be confused for the kind of endpoint sought in this study. However, the recrystallization endpoint is not independent of scan rate or of sample size as is p^c_{H2O} (unpublished data from this laboratory). The equipment used in this study could be used to readily study the kinetics of water catalyzed reactions as a function of p_{H2O} by holding the scanning block in an isothermal condition. Because the water temperature is continuously adjustable, a continuum of p_{H2O} values is accessible; unlike the discrete p_{H2O} values attainable with saturated salt solutions used with the earlier method (Angberg et al., 1992b). Another recent report related to this study describes the use of calorimetry to determine the water content of hydrates (Khankari et al., 1992).

Sensors other than a calorimeter, e.g. humidity and mass, could be used in much the same way the calorimeter is used in this study. The detection limits and sensitivities could be comparable to those of the calorimetric system. However, because a heat conduction calorimeter measures the rate of reaction directly, the instrument described here also provides direct data on the kinetics of water sorption. The time derivative of data from other types of detectors would have to be taken to obtain kinetics by those methods. Because taking derivatives greatly magnifies errors, the calorimetric method is probably preferable to most other methods.

In contrast with equilibrium methods, the conditions of reaction in the method described here mimic what happens in the very early stages of water sorption. Because the amount of water transferred to the sample during an experiment is very small, i.e. a fraction of a mg, only the sample surface reacts. Because of this condition, all of the data demonstrate that water sorption is a linear function of p_{H2O} or relative humidity.

In conclusion, the method described and tested in this study is suitable for rapidly determining the thermodynamics and kinetics of water sorption on a variety of materials. Because of the rapidity of the method, it is suitable for use in quality control and early stages of formulation where p^c_{H2O} data must be obtained in a short time.

Acknowledgements

The authors thank Deann Taylor for assistance in data analysis. Funding was provided by Baxter Healthcare Corporation.

References

Angberg, M., Nyström, C. and Castensson, S., Evaluation of heat-conduction micro-calorimetry in pharmaceutical stability studies. V. A new approach for continuous measurements in abundant water vapor. *Int. J. Pharmaceut.*, 81 (1992a) 153–167.

Angberg, M., Nyström, C. and Castensson, S., Evaluation of heat-conduction micro-calorimetry in pharmaceutical stability studies. VI. Continuous monitoring of the interaction of water vapour with powders and powder mixtures at various relative humidities. *Int. J. Pharmaceut.*, 83 (1992b) 11–23.

Carstensen, J.T., *Pharmaceutics of Solids and Solid Dosage Forms*. Wiley-Interscience, New York, 1977.

Hall, J.R. and Brouillard, R.G., Water vapor pressure calculation. *J. Appl. Physiol.*, 58 (1985) 2090.

Khankari, R.K., Law, D. and Grant, D.J.W., Determination of water content in pharmaceutical hydrates by differential scanning calorimetry. *Int. J. Pharmaceut.*, 82 (1992) 117–127.

Linke, W.F., *Solubilities — Inorganic and metal-organic compounds*. Vol. II, 4th edition, American Chemical Society, Washington, D.C., 1965.

Nyqvist, H., Saturated solutions for maintaining specified relative humidities. *Int. J. Pharm. Tech. Prod. Manufact.*, 4 (1983) 47–48.

Rockland, L.B., Saturated salt solutions for static control of relative humidity between 5°C and 40°C. *Anal. Chem.*, 32 (1960) 1375–1376.

Umprayn, K. and Mendes, R.W., Hygroscopicity and moisture adsorption kinetics of pharmaceutical solids: A review. *Drug Dev. Industr. Pharm.*, 13 (1987) 653–693.

Van Campen, L., Amidon, G.L. and Zografi, G., Moisture sorption kinetics for water-soluble substances I. Theoretical considerations of heat transport control. *J. Pharm. Sci.*, 72 (1983a) 1381–1388.

Van Campen, L., Amidon, G.L. and Zografi, G., Moisture sorption kinetics for water-soluble substances II. Experimental verification of heat transport control. *J. Pharm. Sci.*, 72 (1983b) 1388–1393.

Van Campen, L., Amidon, G.L. and Zografi, G., Moisture sorption kinetics for water-soluble substances III. Theoretical and experimental studies in air. *J. Pharm. Sci.*, 72 (1983c) 1394–1398.

Van Campen, L., Zografi, G. and Carstensen, J.T., An approach to the evaluation of hygroscopicity for pharmaceutical solids. *Int. J. Pharmaceut.*, 5 (1980) 1–18.

Wagman, D.D., Evans, W.H., Parker, V.B., Schumm, R.H., Halow, I., Bailey, S.M., Churney, K.L. and Nuttall, R.L., The NBS tables of chemical thermodynamic properties. *J. Phys. Chem. Ref. Data*, 11, Suppl. 2. (1982).

Weast, R.C., ed., Pressure of Water Below 100°C. In *Handbook of Chemistry and Physics*, 55th edition, CRC Press, Cleveland, OH, 1974a, p. D159.

Weast, R.C., ed., Constant Humidity. In *Handbook of Chemistry and Physics*, 55th edition, CRC Press, Cleveland, OH, 1974b, p. E-46.